PAUL SCHERRER INSTITUT PSI

Bayesian Calibration and Sensitivity Analysis of Non-Proportional Scintillation Models for Airborne Gamma-Ray Spectrometry Applications

Zurich PhD Seminar 2023, January 26th

David Breitenmoser
Department of Radiation Safety and Security,
Paul Scherrer Institute, 5232 PSI Villigen, Switzerland
Supervision: Dr. Gernot Butterweck
Prof. Dr. Klaus Stefan Kirch

Funding

Schweizerische Eidgenossenschaft
Confédération suisse
Confederazione Svizzera
Confederaziun svizra

Swiss Confederation

Eidgenössisches Nuklearsicherheitsinspektorat ENSI
Inspection fédérale de la sécurité nucléaire IFSN
Ispettorato federale della sicurezza nucleare IFSN
Swiss Federal Nuclear Safety Inspectorate ENSI

contract no. CTR00836

Collaboration

Nationale Alarmzentrale
Centrale nationale d'alarme
Centrale nazionale d'allarme
Centrala naziunala d'alarm

Schweizer Armee
Armée suisse
Esercito svizzero
Swiss Armed Forces

CERN

MIRION TECHNOLOGIES

Together ahead. RUAG

Overview

1. **Introduction**
2. Methodology
3. Results
4. Conclusion

Airborne Gamma-Ray Spectrometry

PAUL SCHERRER INSTITUT PSI

Airborne Gamma-Ray Spectrometry

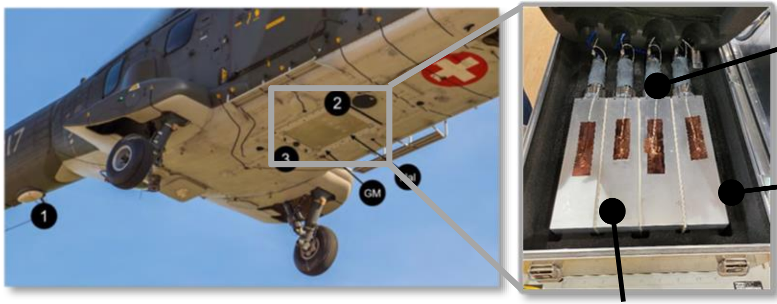

Airborne Gamma-Ray Spectrometry

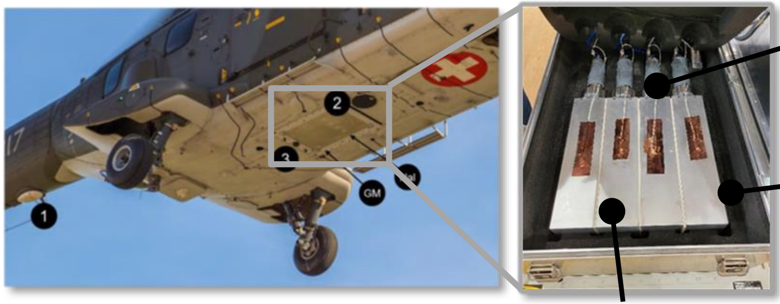

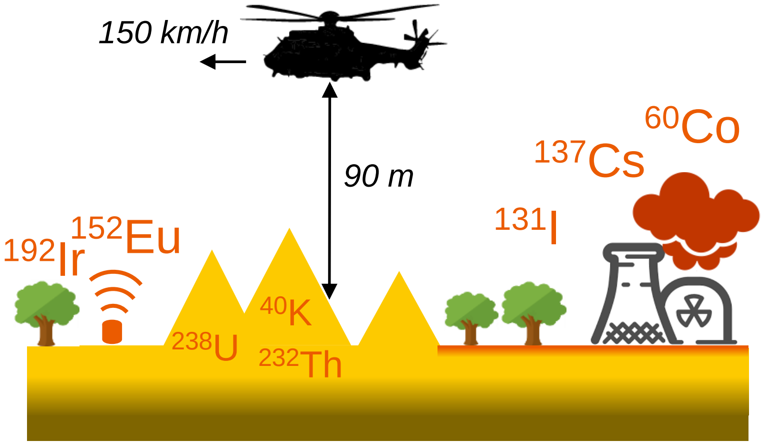

Airborne Gamma-Ray Spectrometry

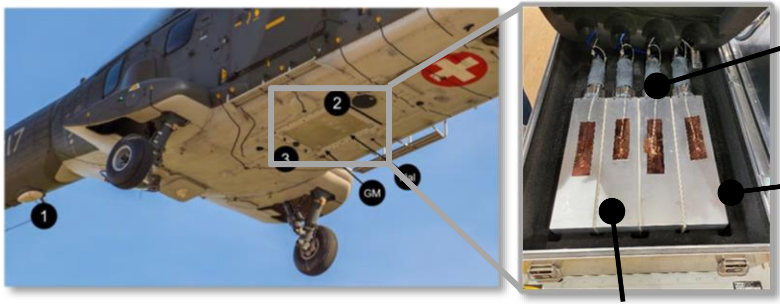

Photo-multiplier

Vibration damping foam

4 x NaI(Tl) scintillation crystal (10 x 10 x 40 cm³)

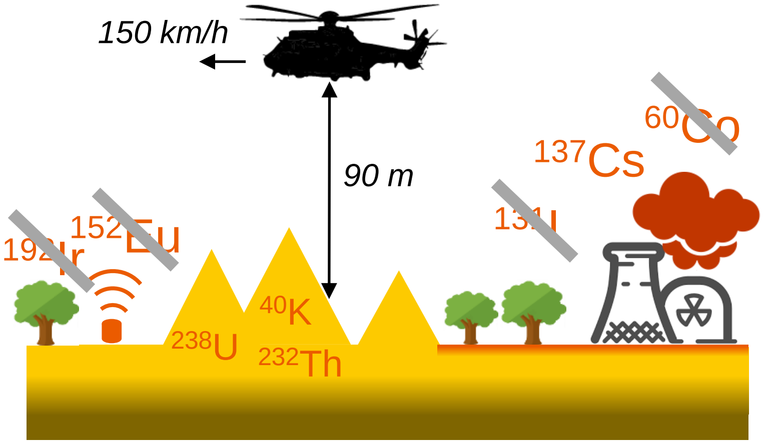

Challenge: No identification & quantification of man-made sources

PAUL SCHERRER INSTITUT

Airborne Gamma-Ray Spectrometry

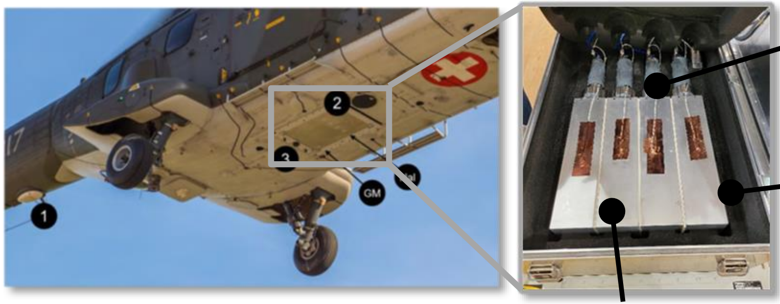

Photo-multiplier

Vibration damping foam

4 x NaI(Tl) scintillation crystal (10 x 10 x 40 cm³)

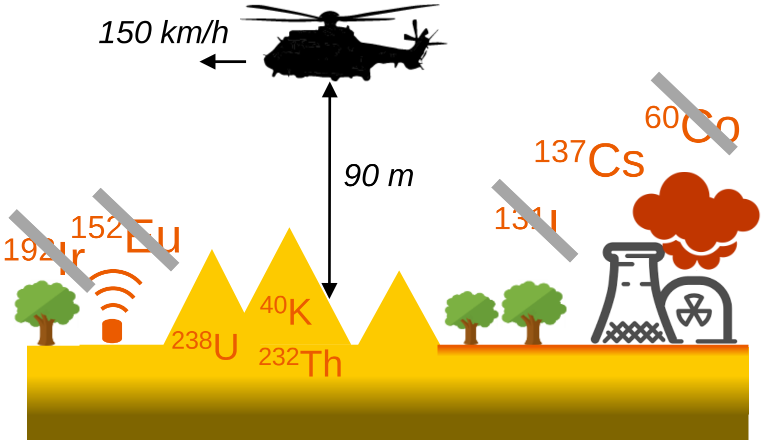

Challenge: No identification & quantification of man-made sources

Scope: Numerical calibration by Monte Carlo methods

Detector Response Model

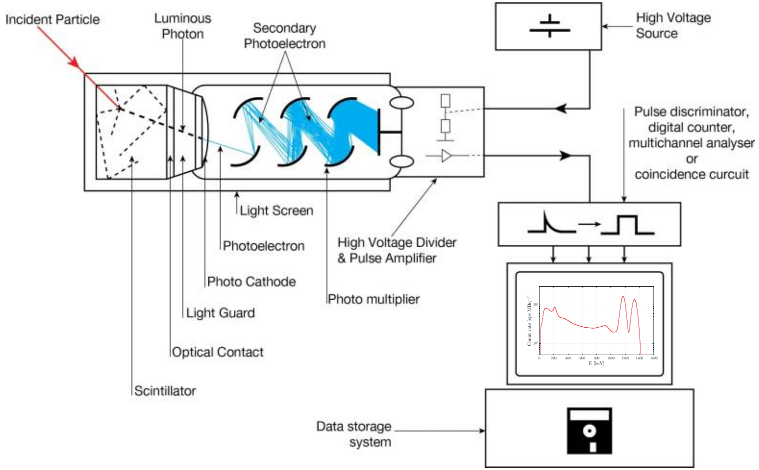

Detector Response Model

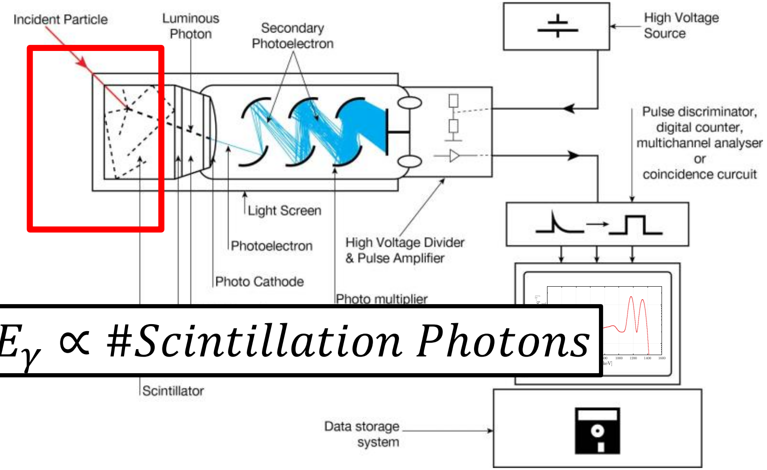

$$E_\gamma \propto \#Scintillation\ Photons$$

Detector Response Model

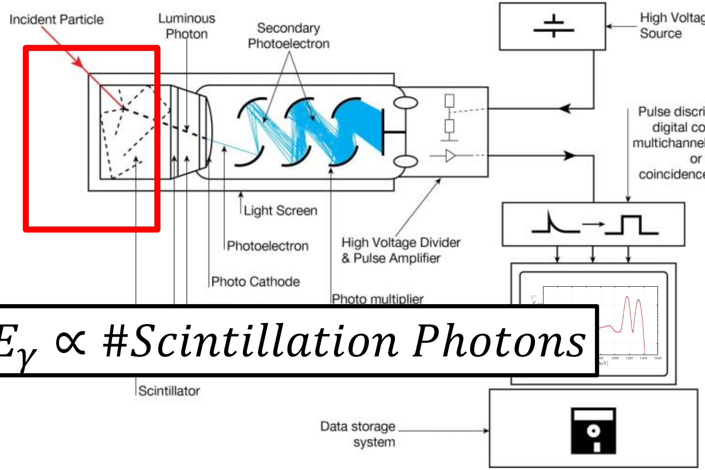

$E_\gamma \propto$ #Scintillation Photons

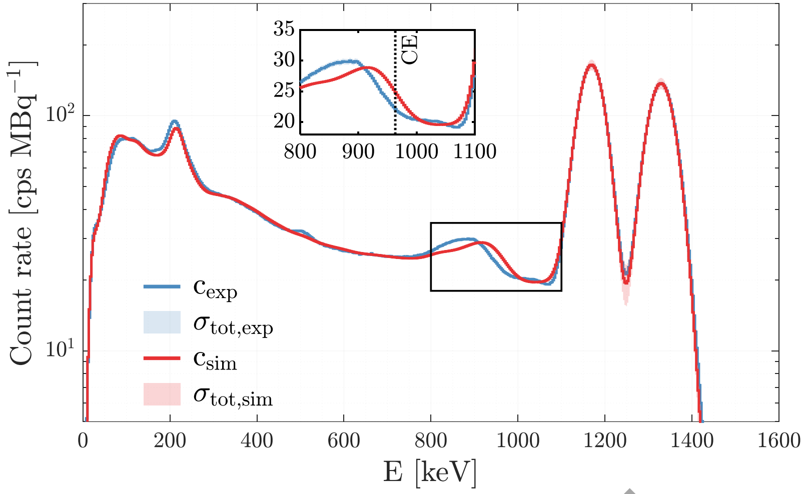

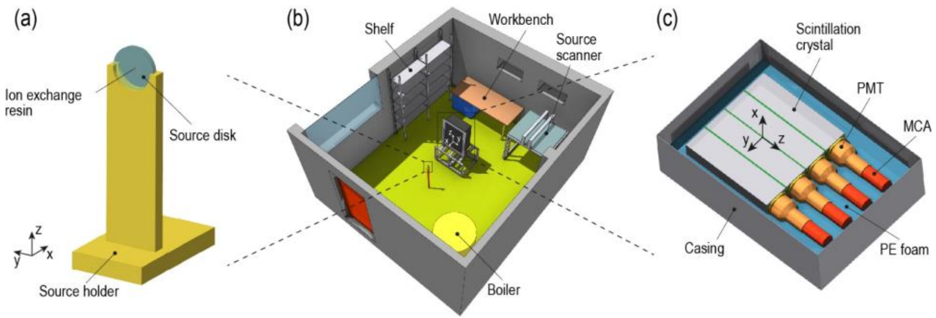

FLUKA

D. Breitenmoser et al., "Experimental and Simulated Spectral Gamma-Ray Response of a NaI(Tl) Scintillation Detector used in Airborne Gamma-Ray Spectrometry" *Advances in Geosciences* **57**, 89–107 (2022).

Overview

1. Introduction
2. **Methodology**
3. Results
4. Conclusion

2. Model Parametrization

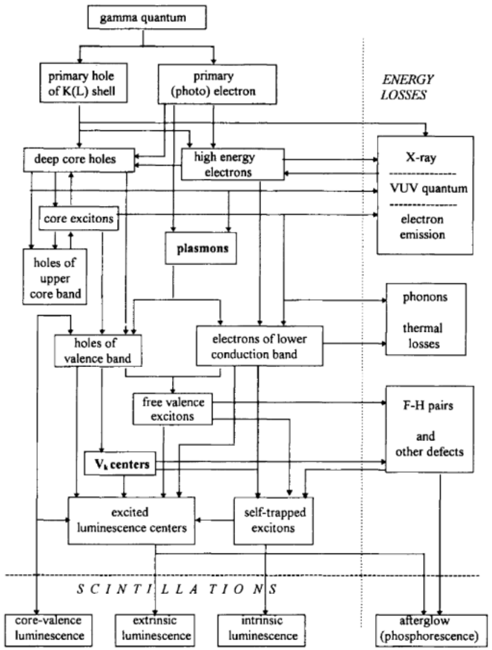

P. A. Rodnyi, *Physical Processes in Inorganic Scintillators* 1st edn (CRC Press, New York, USA, 1997).

2. Model Parametrization

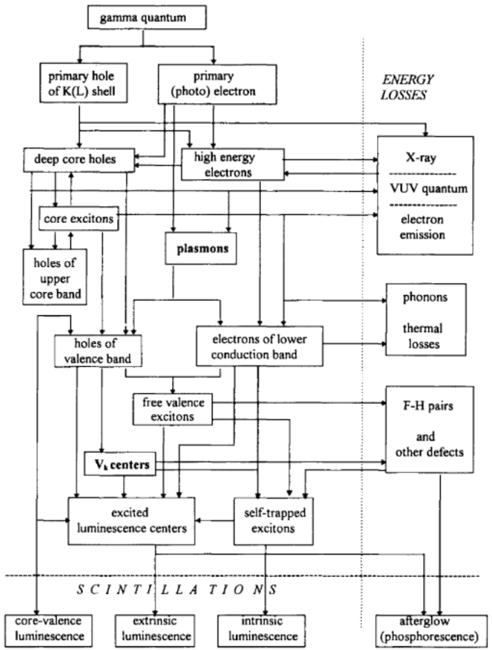

P. A. Rodnyi, *Physical Processes in Inorganic Scintillators* 1st edn (CRC Press, New York, USA, 1997).

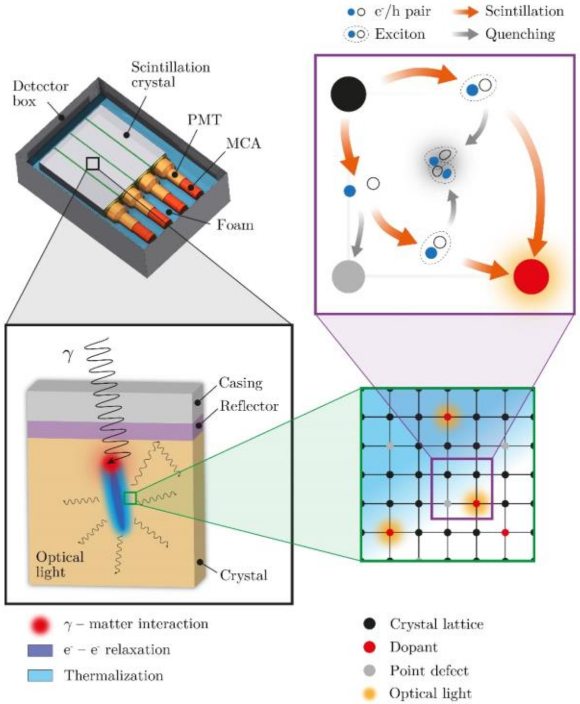

$$L(S|\boldsymbol{x}) \propto \frac{1 - x_{e/h} e^{\left[\frac{S}{x_{Ons}} e^{\left(\frac{x_{Tr}}{S}\right)}\right]}}{1 - \frac{S}{x_{Birks}}}$$

L: Relative light yield

S: Electronic stopping power

x: Model parameters

P. R. Beck et al., “Nonproportionality of Scintillator Detectors. V. Comparing the Gamma and Electron Response,” *IEEE Trans. Nucl. Sci.* **62**(3), 1429–1436 (2015).

2. Forward Simulation

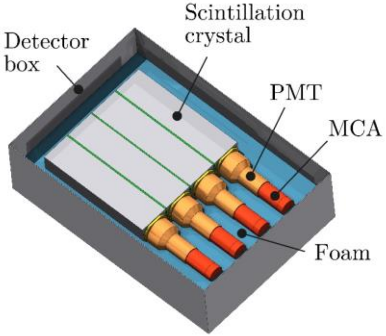

$+ \; L(S|\boldsymbol{x})$

FLUKA

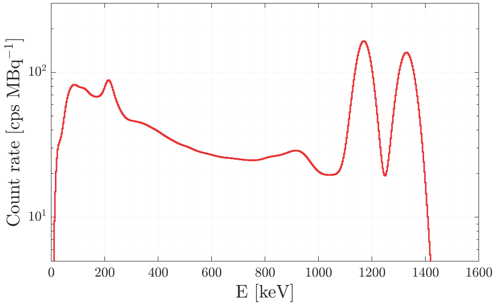

2. Bayesian Calibration

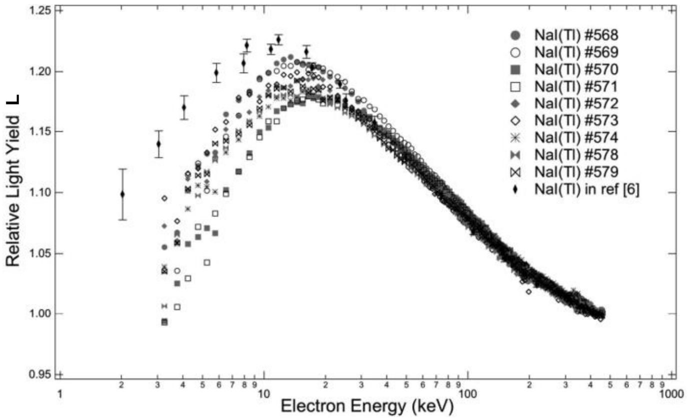

G. Hull et al., "Measurements of NaI(Tl) electron response: Comparison of different samples," *IEEE Trans. Nucl. Sci.* **56**(1), 331–336 (2009)

2. Bayesian Calibration

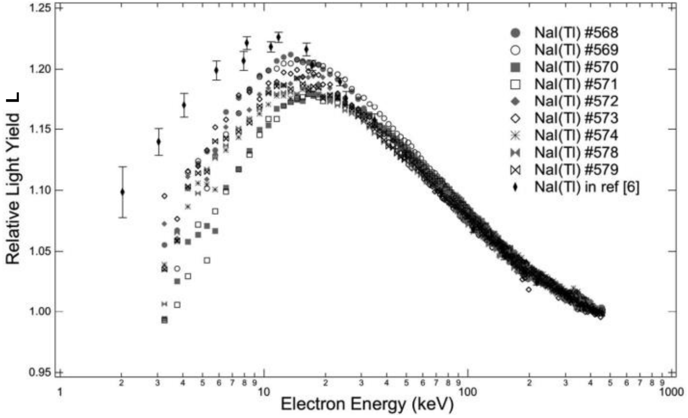

G. Hull et al., "Measurements of NaI(Tl) electron response: Comparison of different samples," *IEEE Trans. Nucl. Sci.* **56**(1), 331–336 (2009)

x → **System Model** → **y**

→ Forward Problem

2. Bayesian Calibration

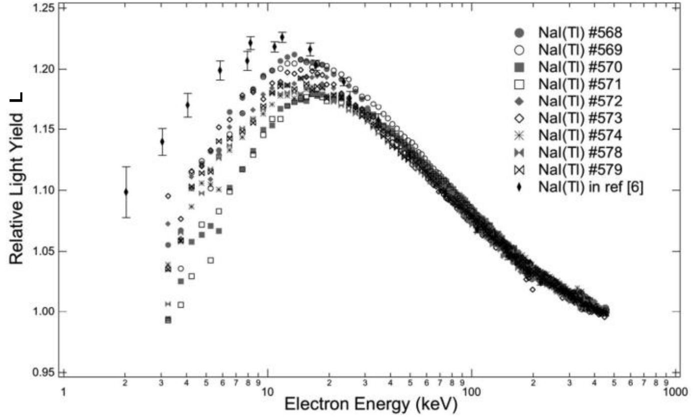

G. Hull et al., “Measurements of NaI(Tl) electron response: Comparison of different samples,” *IEEE Trans. Nucl. Sci.* **56**(1), 331–336 (2009)

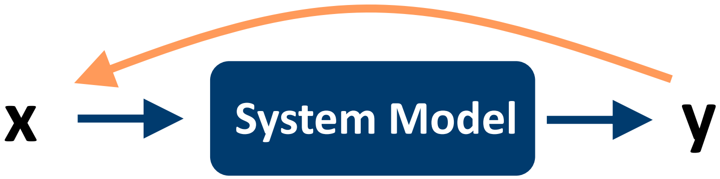

Forward Problem

Inverse Problem

2. Bayesian Calibration

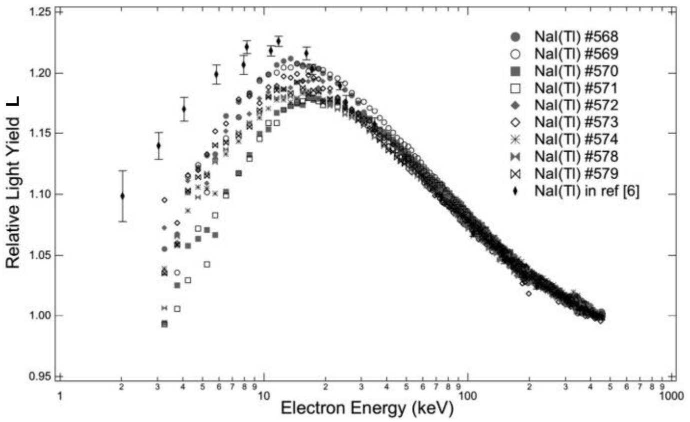

G. Hull et al., "Measurements of NaI(Tl) electron response: Comparison of different samples," *IEEE Trans. Nucl. Sci.* **56**(1), 331–336 (2009)

Ill-posed problem:
1) No solution guaranteed
2) No unique solution guaranteed
3) Discontinuous solution possible

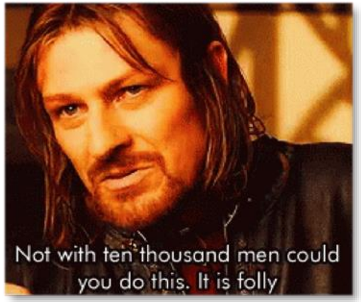

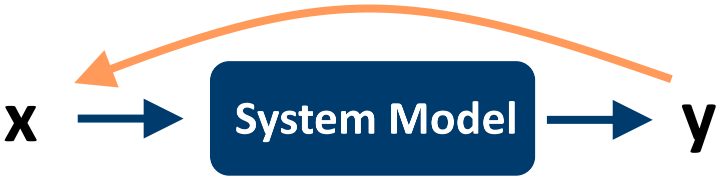

Forward Problem

Inverse Problem

2. Bayesian Calibration

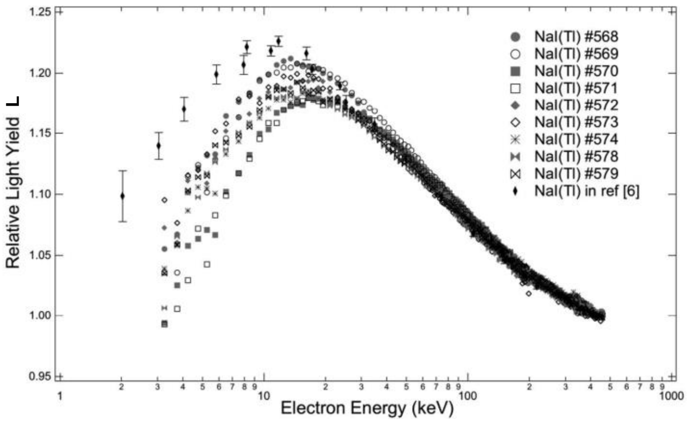

G. Hull et al., "Measurements of NaI(Tl) electron response: Comparison of different samples," *IEEE Trans. Nucl. Sci.* **56**(1), 331–336 (2009)

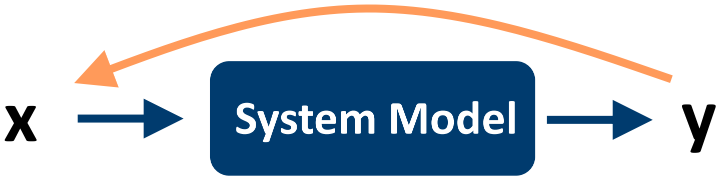

Forward Problem

Inverse Problem

Ill-posed problem:

1) No solution guaranteed
2) No unique solution guaranteed
3) Discontinuous solution possible

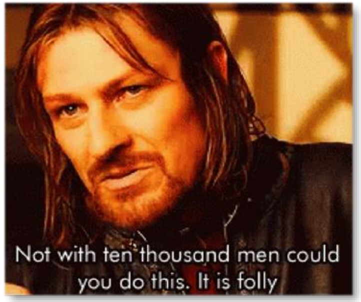

Bayesian Calibration

$$\pi(x|y) = \frac{\mathcal{L}(x|y)\pi(x)}{\int \mathcal{L}(x|y)\pi(x)dx}$$

$\mathcal{L}(x|y)$ Likelihood function

$\pi(x)$ Prior probability density

2. Surrogate Modelling

Computation time on computer cluster:

1) Bayesian calibration ≈ 10^5 model evaluations
2) 1 Model evaluation ≈ 1h computation time
3) #Calibrations ≈ 4x

2. Surrogate Modelling

Computation time on computer cluster:
1) Bayesian calibration ≈ 10^5 model evaluations
2) 1 Model evaluation ≈ 1h computation time
3) #Calibrations ≈ 4x

= 46 years

2. Surrogate Modelling

Computation time on computer cluster:

1) Bayesian calibration ≈ 10^5 model evaluations
2) 1 Model evaluation ≈ 1h computation time
3) #Calibrations ≈ 4x

= 46 years

Machine Learning

PCE-PCA Model:

$$\boldsymbol{Y} \approx \mathcal{M}^{\mathrm{PC}}(\boldsymbol{X}_{\mathcal{M}}) \overset{\mathrm{def}}{=} \boldsymbol{Y}^{\mathrm{PCA+PCE}} = \boldsymbol{\mu}_Y + \sum_{p=1}^{N'} \left(\sum_{\alpha \in \mathcal{A}_p} \widetilde{a}_{p,\alpha} \Psi_{\alpha}(\boldsymbol{X}_{\mathcal{M}}) \right) \boldsymbol{\phi}_p$$

+ global sensitivity Sobol indices for free
+ Small prediction errors < 1%
+ excellent evaluation time ~100µs

= 40 s

E. Torre et al., "Data-driven polynomial chaos expansion for machine learning regression" *Journal of Computational Physics* **388**, 601–623 (2019)

2. Radiation Measurements

Measurement Set-Up

Mass Model

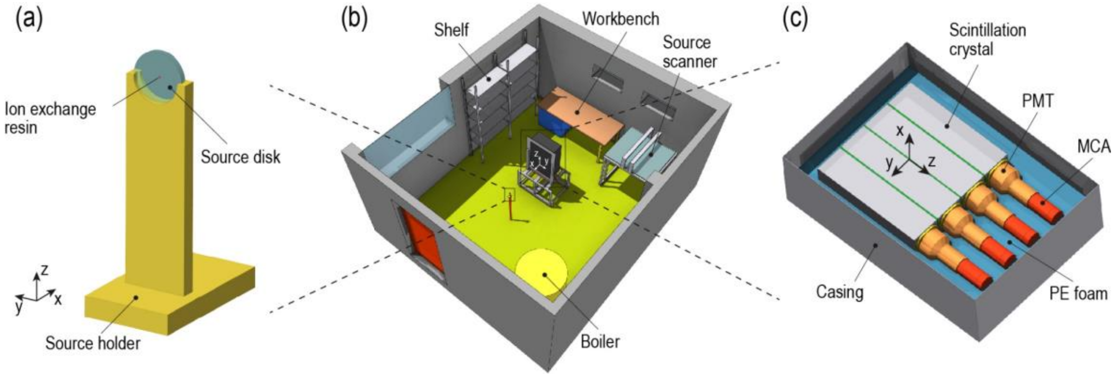

D. Breitenmoser et al., “Experimental and Simulated Spectral Gamma-Ray Response of a NaI(Tl) Scintillation Detector used in Airborne Gamma-Ray Spectrometry” *Advances in Geosciences* **57**, 89–107 (2022).

Radiation Source

Source [−]	Half life[a] [d]	Activity[b] [Bq]	Photon energy[c] [keV]
^{57}Co	$2.7180(5) \cdot 10^2$	$1.11(2) \cdot 10^5$	122.0607(1)
			136.4736(3)
^{60}Co	$1.9252(3) \cdot 10^3$	$3.08(5) \cdot 10^5$	1173.228(3)
			1332.492(4)
^{88}Y	$1.0663(2) \cdot 10^2$	$6.8(1) \cdot 10^5$	898.042(3)
			1836.06(1)
^{109}Cd	$4.61(1) \cdot 10^2$	$7.4(2) \cdot 10^4$	88.0336(1)
^{133}Ba	$3.850(2) \cdot 10^3$	$2.15(3) \cdot 10^5$	80.997(1)
			276.400(1)
			302.8510(6)
			356.0134(6)
			383.848(1)
^{137}Cs	$1.098(3) \cdot 10^4$	$2.27(3) \cdot 10^5$	661.657(3)
^{152}Eu	$4.939(6) \cdot 10^3$	$1.97(3) \cdot 10^4$	121.7817(3)
			244.6975(8)
			344.279(1)
			411.116(1)
			443.965(3)
			778.904(2)
			867.373(3)
			964.08(2)
			1085.87(2)
			1112.069(3)
			1408.006(3)

Overview

1. Introduction
2. Methodology
3. **Results**
4. Conclusion

3. Results – Posterior Distribution

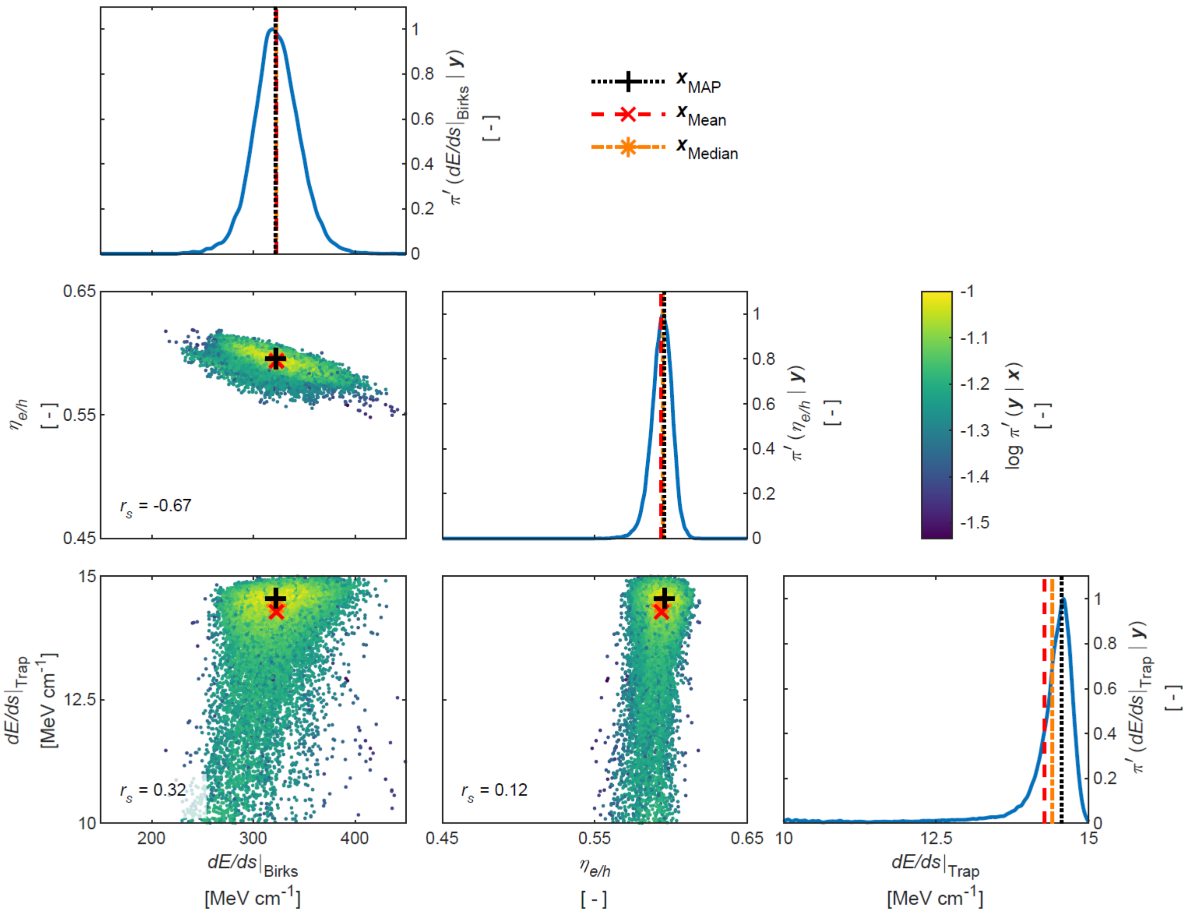

3. Results – Emulator Predictions

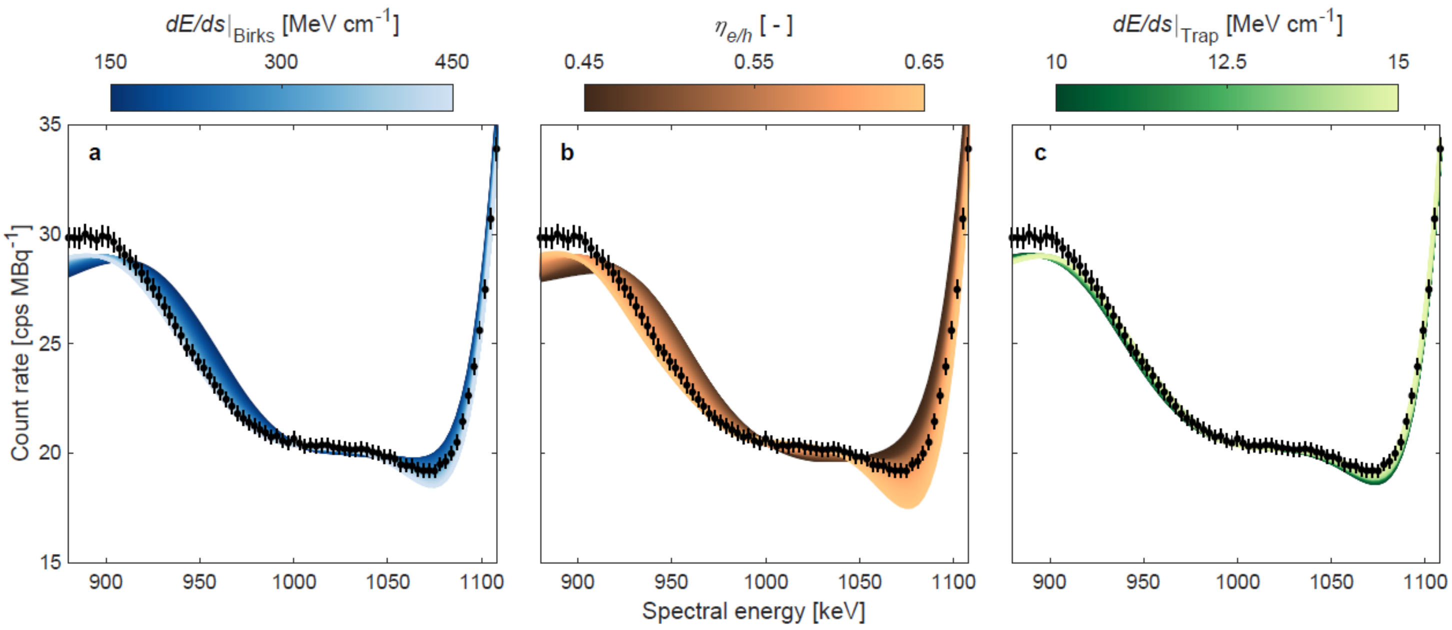

3. Results – Posterior Prediction & Sensitivity

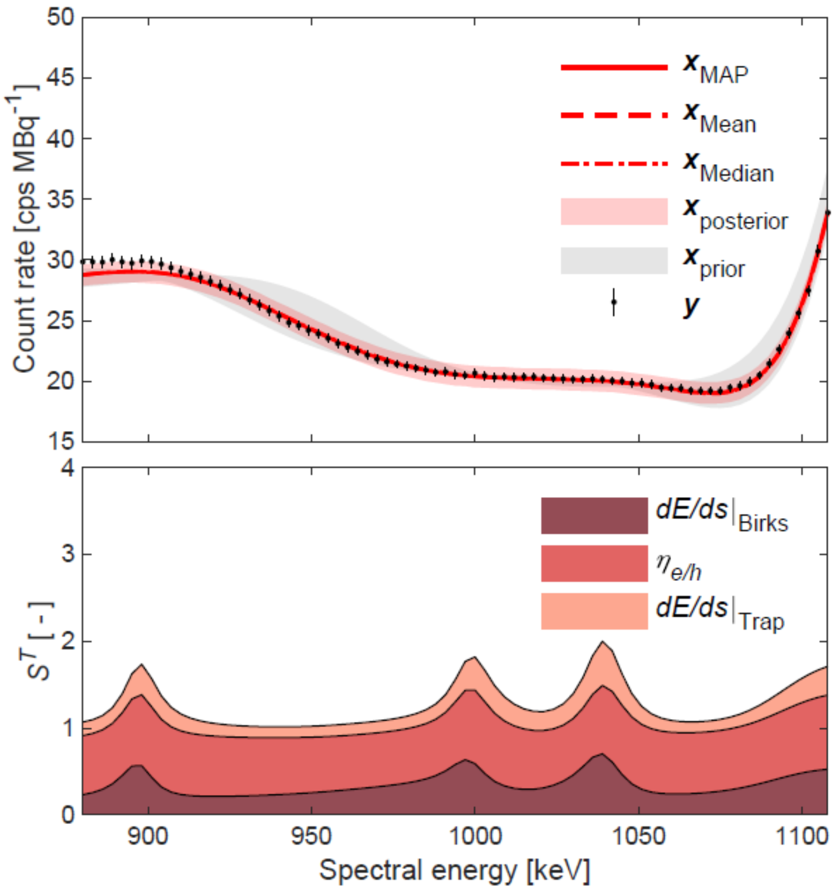

3. Results – Intrinsic Resolution

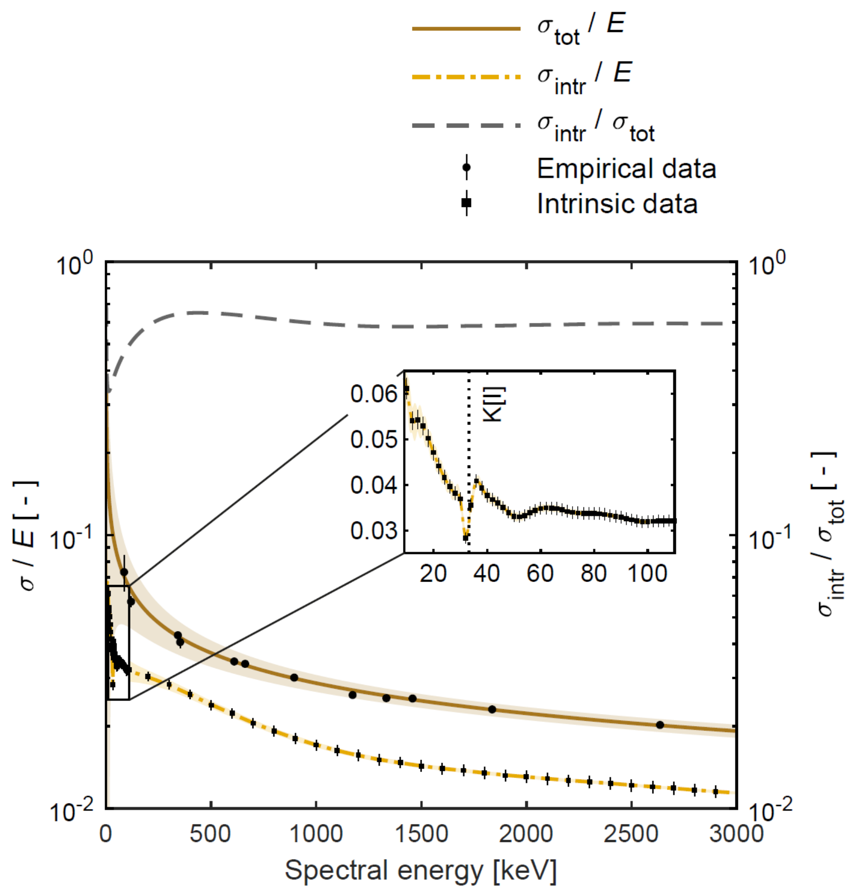

3. Results

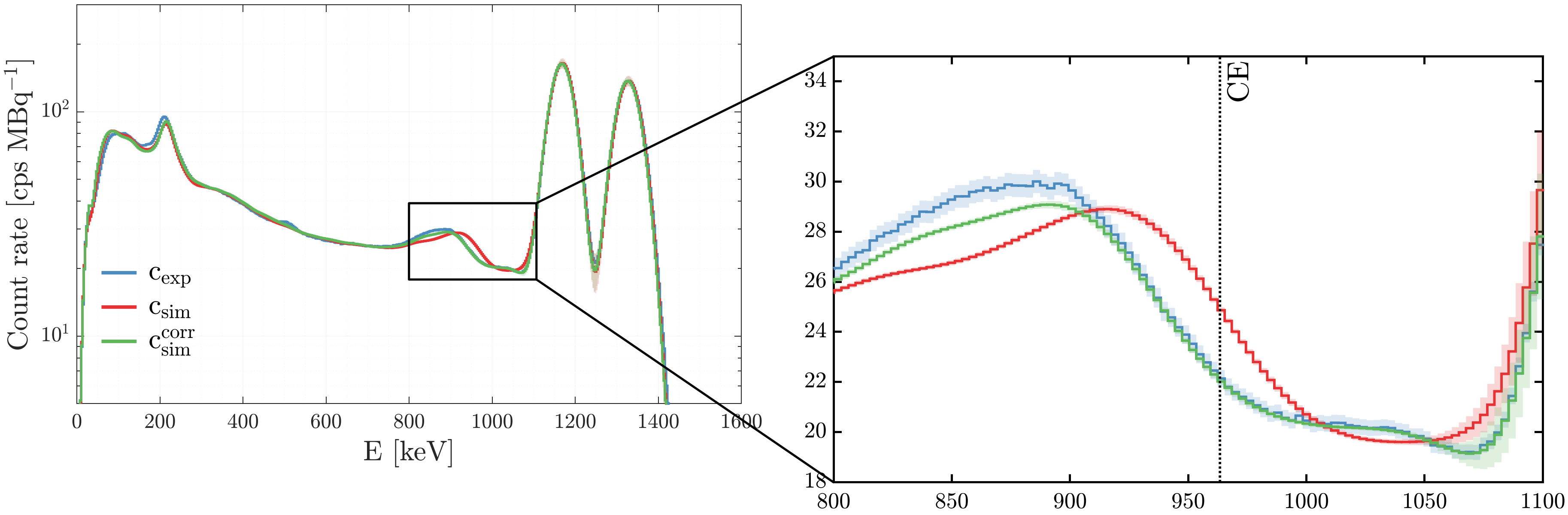

Count rate [cps MBq^{-1}]
10^2
10^1
0
200
400
600
800
1000
1200
1400
1600
E [keV]
c_{exp}
c_{sim}
c_{sim}^{corr}
34
32
30
28
26
24
22
20
18
800
850
900
950
1000
1050
1100
CE

3. Results

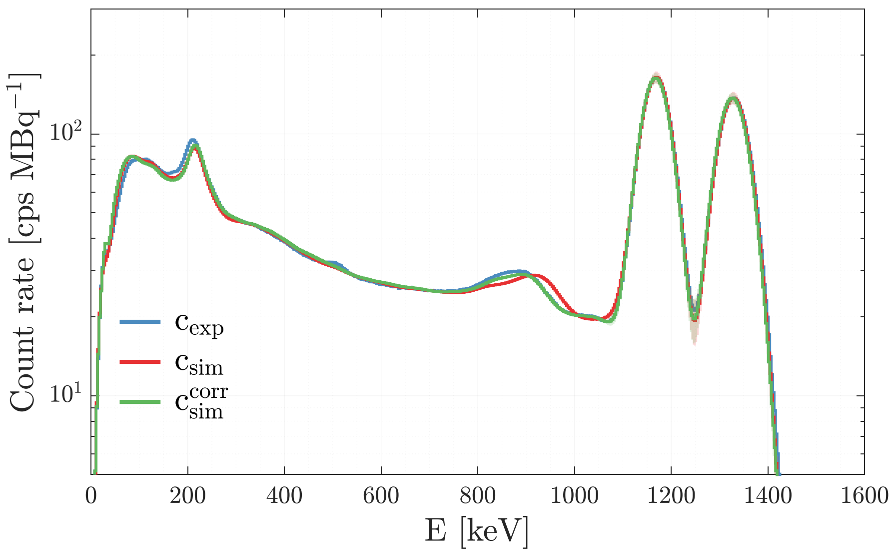

Count rate [cps MBq^{-1}]
10^2
10^1
c_{exp}
c_{sim}
c_{sim}^{corr}
0
200
400
600
800
1000
1200
1400
1600
E [keV]

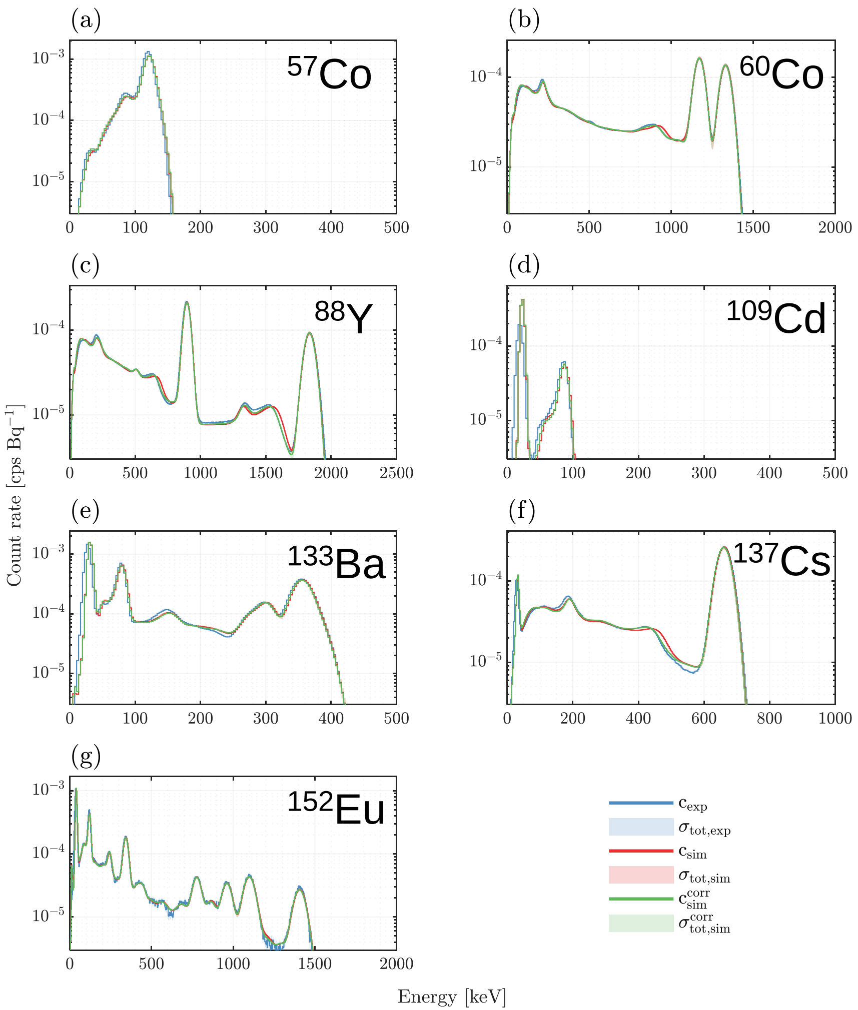

(a) ^{57}Co
(b) ^{60}Co
(c) ^{88}Y
(d) ^{109}Cd
(e) ^{133}Ba
(f) ^{137}Cs
(g) ^{152}Eu
Count rate [cps Bq^{-1}]
Energy [keV]
c_{exp}
$\sigma_{tot,exp}$
c_{sim}
$\sigma_{tot,sim}$
c_{sim}^{corr}
$\sigma_{tot,sim}^{corr}$

3. Results

Detector Response Simulations

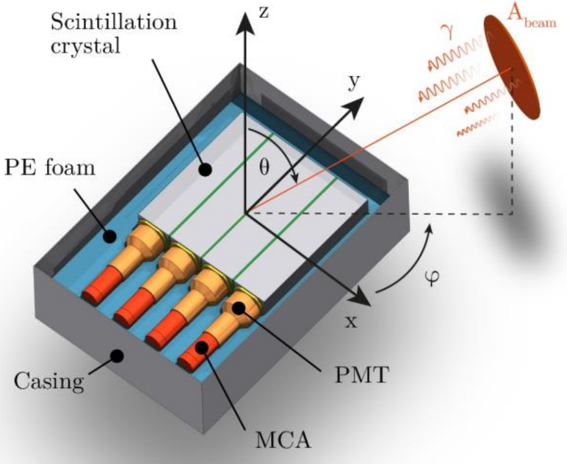

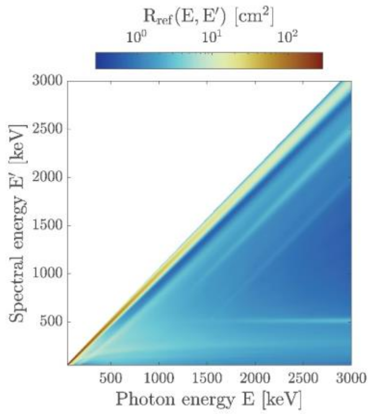

- 7980 design
- > 9000 CPU hours
- 50 – 3000 keV
- online non-proportional scintillation
- rigorous uncertainty propagation

Detector Response Function:

$$R(E, E', \varphi, \theta) \ [\mathrm{cm}^2]$$

E photon energy [keV]
E' detected energy [keV]
φ azimuth angle [°]
θ polar angle[°]

3. Results

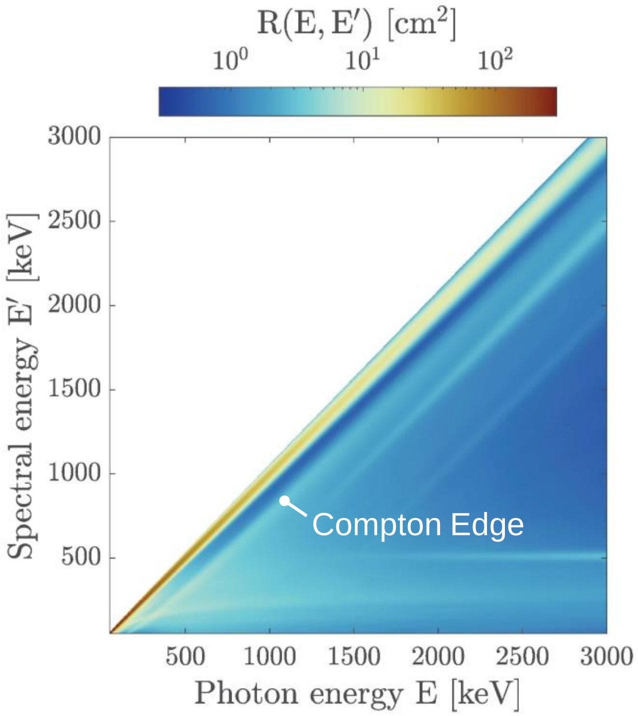

Energy Dispersion
(θ = φ = 0°)

PAUL SCHERRER INSTITUT PSI

3. Results

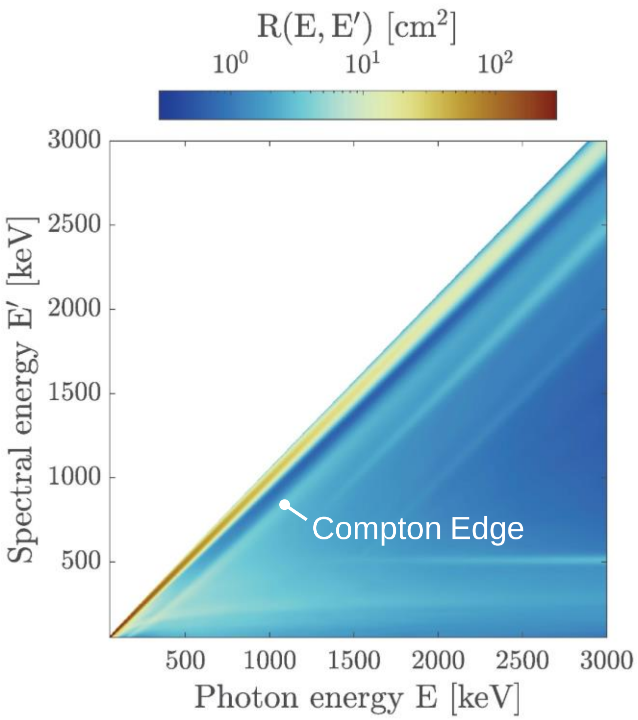

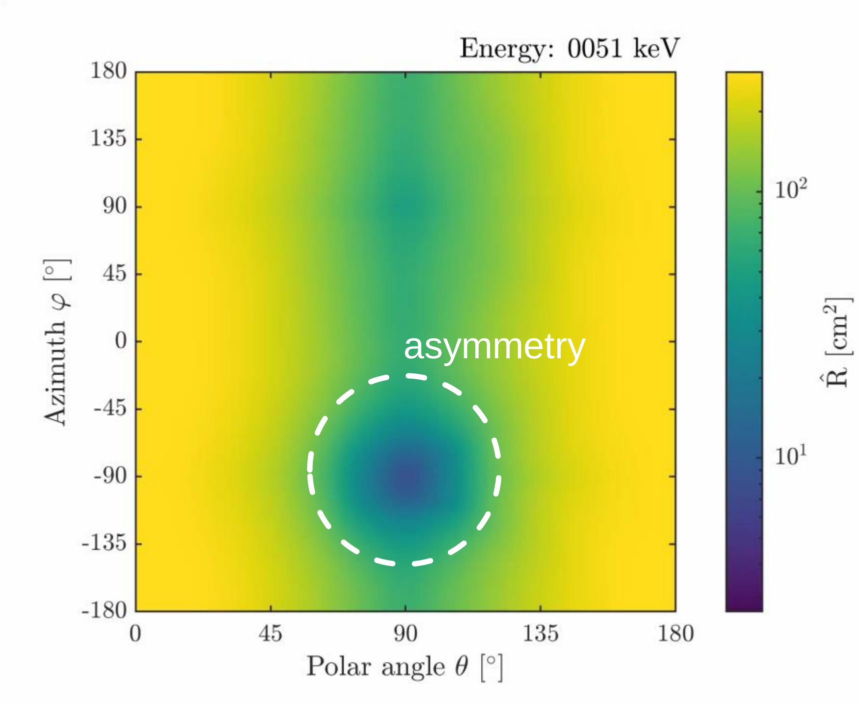

Energy Dispersion
(θ = φ = 0°)

Angular Sensitivity
(E = E′)

3. Results

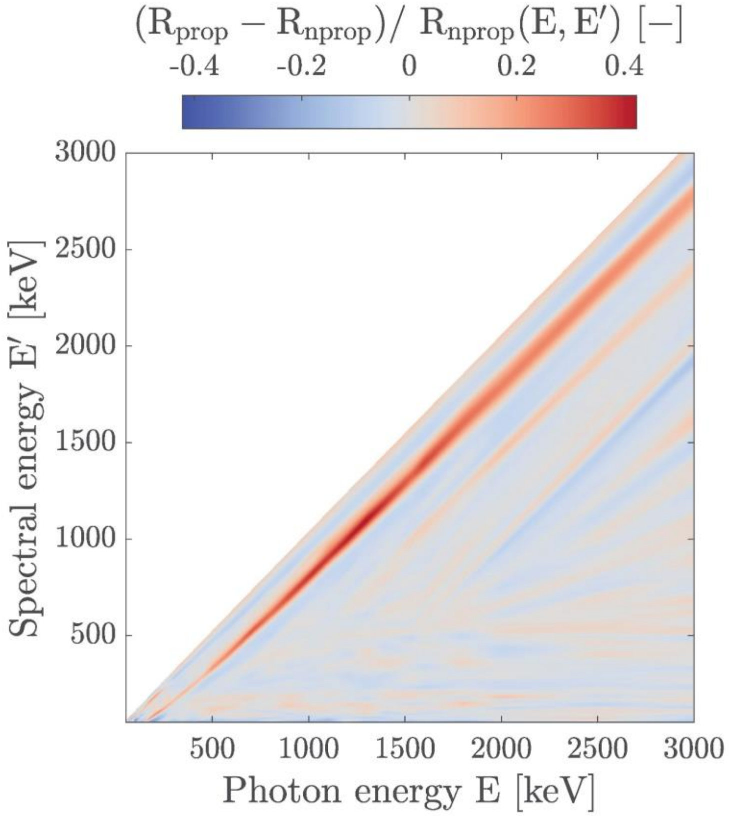

($\theta = \varphi = 0°$)

Overview

1. Introduction
2. Methodology
3. Results
4. **Conclusion**

PAUL SCHERRER INSTITUT

4. Conclusion

✓ Novel method: reliable, easy & applicable during detector deployment

4. Conclusion

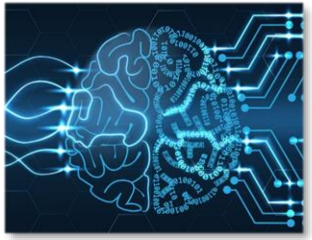

- ✓ Novel method: reliable, easy & applicable during detector deployment
- ✓ Thanks to sparse machine learning models: very fast and global sensitivity analysis for free

4. Conclusion

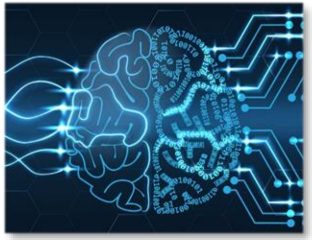

- Novel method: reliable, easy & applicable during detector deployment
- Thanks to sparse machine learning models: very fast and global sensitivity analysis for free
- AGRS: all the nuclides we want
  Very important for radiation protection applications!

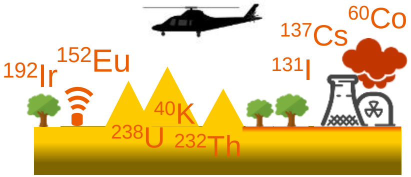

4. Conclusion

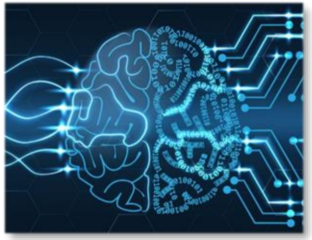

✓ Novel method: reliable, easy & applicable during detector deployment

✓ Thanks to sparse machine learning models: very fast and global sensitivity analysis for free

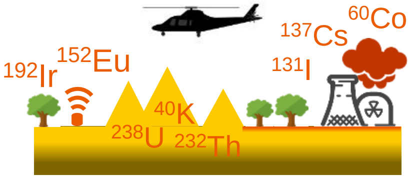

✓ AGRS: all the nuclides we want
Very important for radiation protection applications!

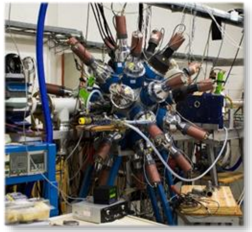

✓ Can be used for any inorganic scintillator

PAUL SCHERRER INSTITUT

4. Conclusion

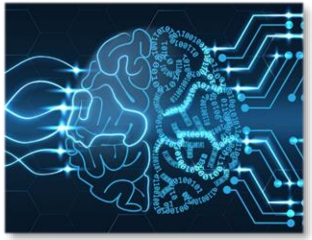

- ✓ Novel method: reliable, easy & applicable during detector deployment

- ✓ Thanks to sparse machine learning models: very fast and global sensitivity analysis for free

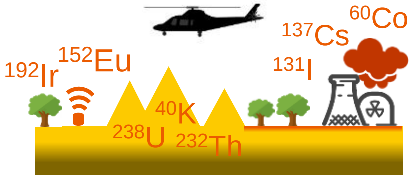

- ✓ AGRS: all the nuclides we want
  Very important for radiation protection applications!

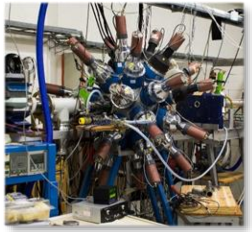

- ✓ Can be used for any inorganic scintillator

- ✓ Open source: You can have it!

PAUL SCHERRER INSTITUT PSI

Wir schaffen Wissen – heute für morgen

Thank you for your attention!

I'm happy to answer now your questions…

Funding

This work was partly funded by the Swiss Federal Nuclear Safety Inspectorate ENSI, contract no. CTR00836.

Collaboration

Schweizerische Eidgenossenschaft
Confédération suisse
Confederazione Svizzera
Confederaziun svizra

Swiss Confederation

Eidgenössisches Nuklearsicherheitsinspektorat ENSI
Inspection fédérale de la sécurité nucléaire IFSN
Ispettorato federale della sicurezza nucleare IFSN
Swiss Federal Nuclear Safety Inspectorate ENSI

Nationale Alarmzentrale
Centrale nationale d'alarme
Centrale nazionale d'allarme
Centrala naziunala d'alarm

CERN

Schweizer Armee
Armée suisse
Esercito svizzero
Swiss Armed Forces

MIRION TECHNOLOGIES

Together ahead. RUAG

Additional Slides

Appendix

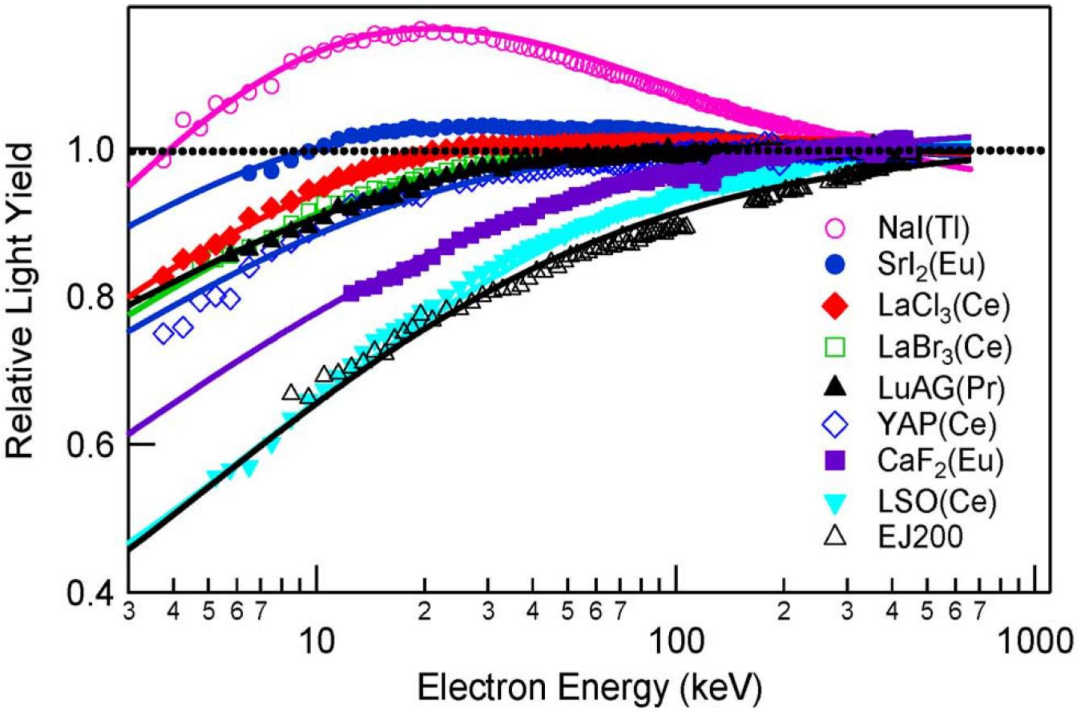

W. W. Moses *et al.*, “The origins of scintillator non-proportionality,” *IEEE Trans. Nucl. Sci.*, vol. 59, no. 5 PART 2, pp. 2038–2044, 2012.

Appendix

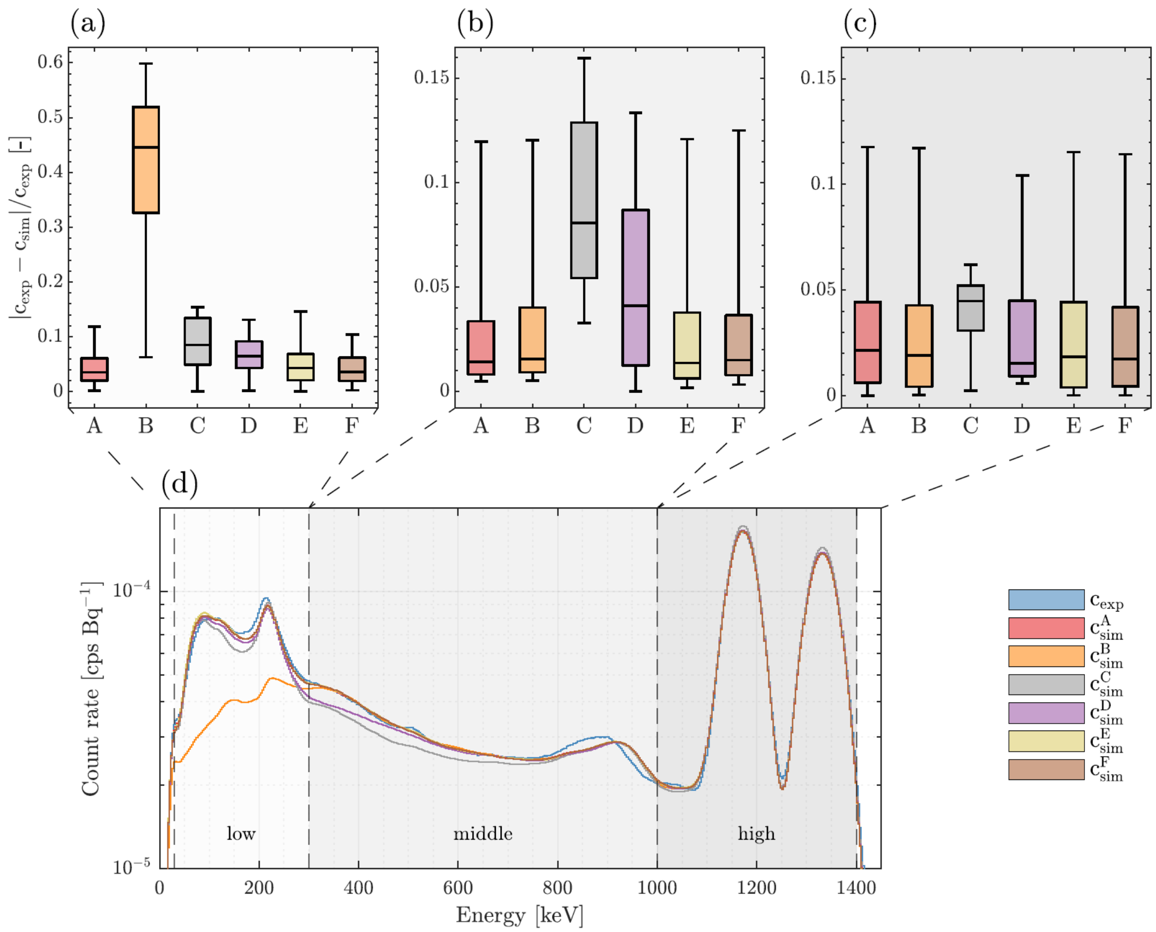

A	Reference
B	No room (floor, walls, ceiling)
C	No detector box (casing, PMT, MCA, foam,…)
D	No source materials (disk, source holder, tripod)
E	No additionals installations (shelves, working bench, boiler)
F	MgO reflector

Appendix

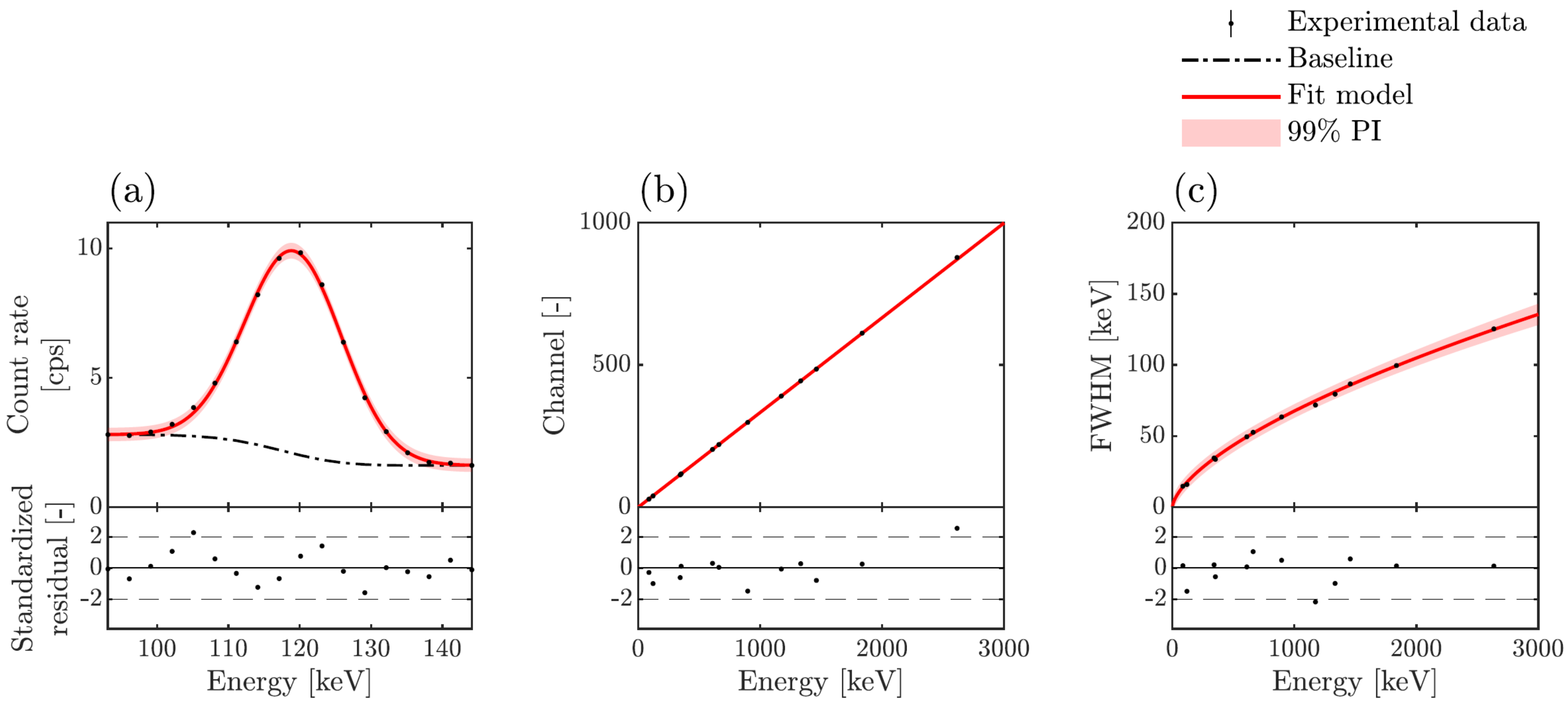

Experimental data
Baseline
Fit model
99% PI
(a)
(b)
(c)
Count rate [cps]
Standardized residual [-]
Channel [-]
FWHM [keV]
Energy [keV]
Energy [keV]
Energy [keV]

Appendix

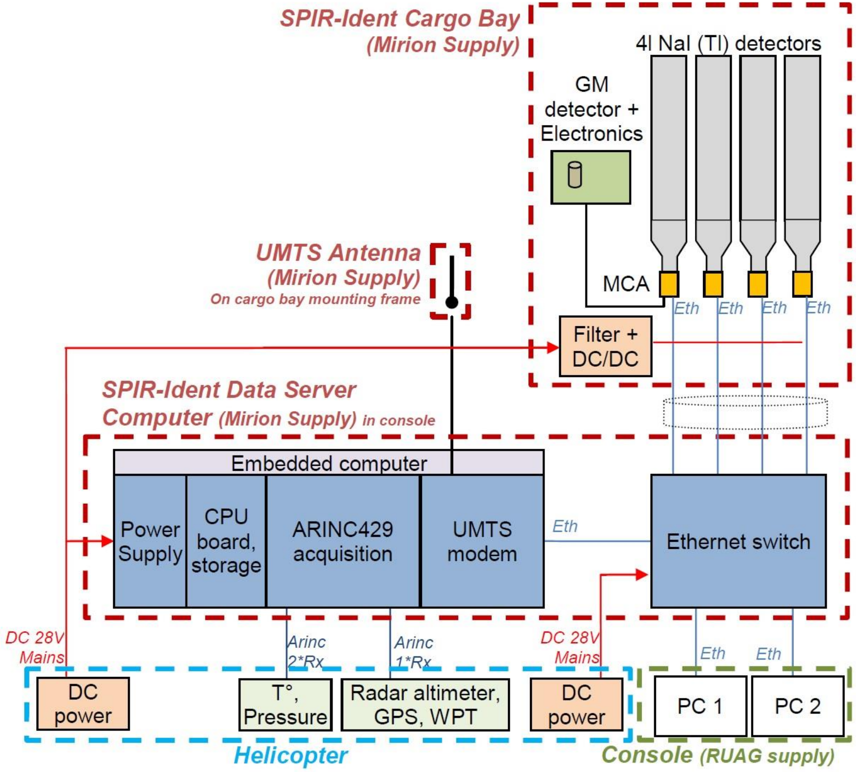

SPIR-Ident Cargo Bay
(Mirion Supply)
4l NaI (Tl) detectors
GM detector + Electronics
MCA
Eth
Eth
Eth
Eth
Filter + DC/DC
UMTS Antenna
(Mirion Supply)
On cargo bay mounting frame
SPIR-Ident Data Server Computer (Mirion Supply) in console
Embedded computer
Power Supply
CPU board, storage
ARINC429 acquisition
UMTS modem
Eth
Ethernet switch
DC 28V Mains
Arinc 2*Rx
Arinc 1*Rx
DC 28V Mains
Eth
Eth
DC power
T°, Pressure
Radar altimeter, GPS, WPT
DC power
PC 1
PC 2
Helicopter
Console (RUAG supply)

PAUL SCHERRER INSTITUT PSI

Appendix

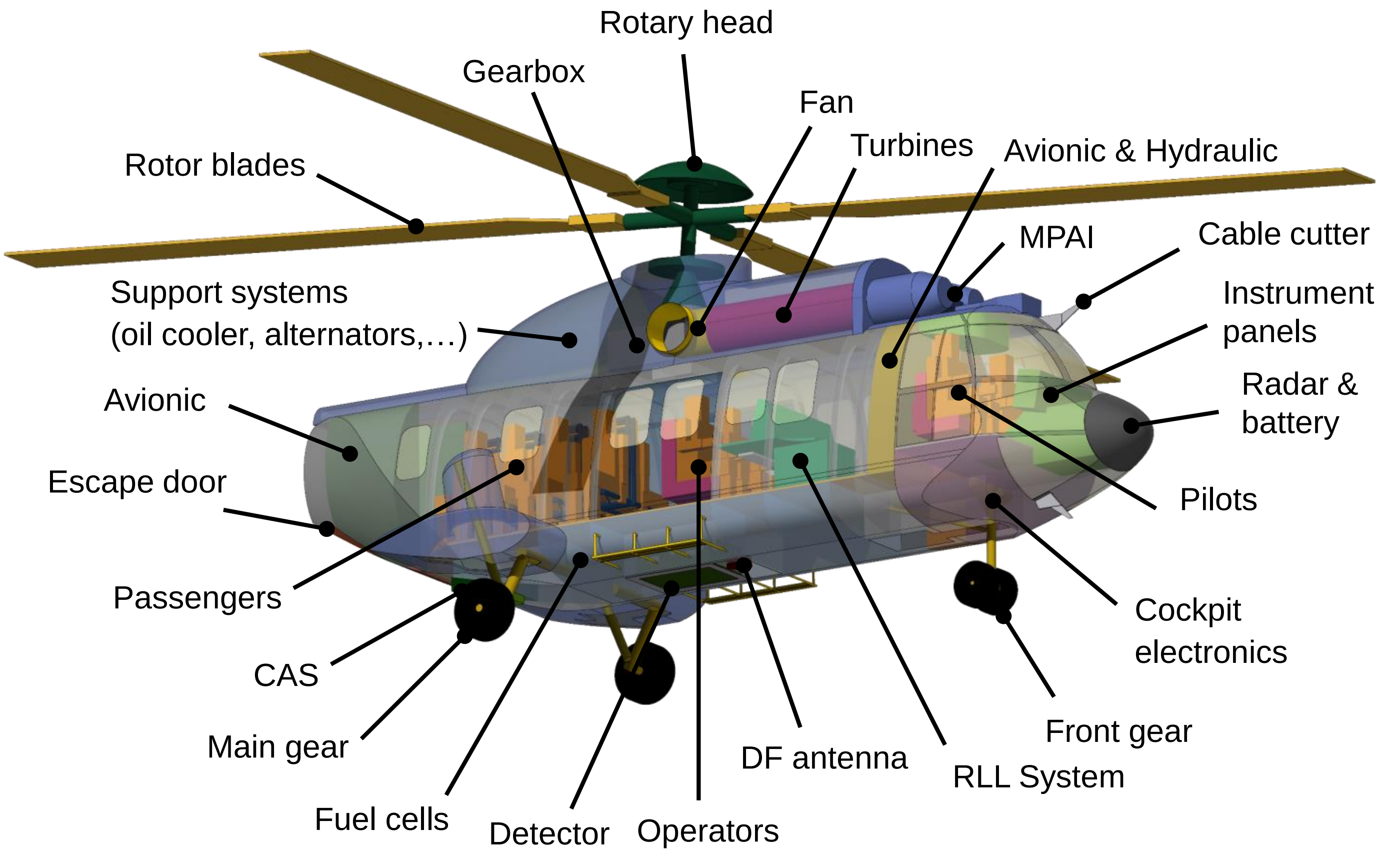

Modelling Principles

- High-fidelity modelling in near-field around validated detector
- Simplified geometries in far-field (overall mass density and opacity preserved)
- Detailed elemental composition for all materials
- Advanced quadric surfaces to fit complex aircraft hull
- Dynamic modelling of gears, crew comp., fuel cells & rotor blades

Appendix

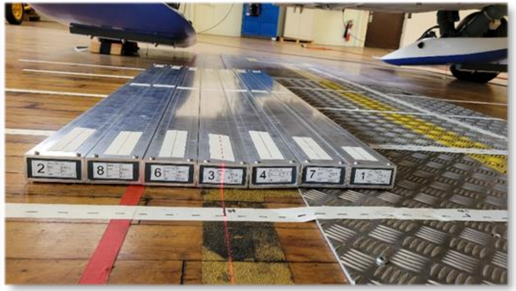

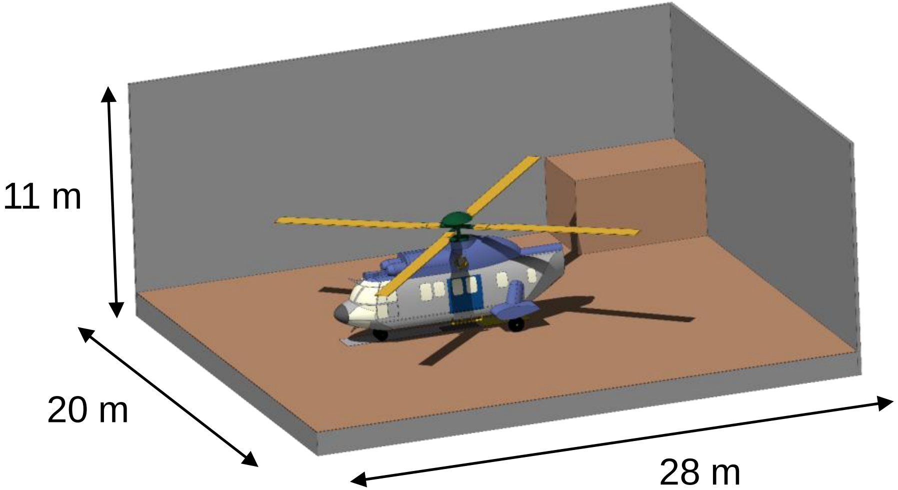

Appendix

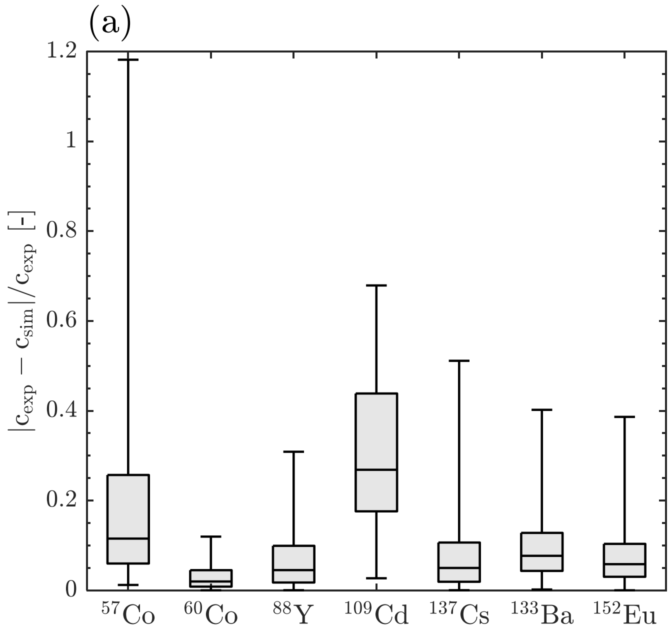

(a)
1.2
1
0.8
0.6
0.4
0.2
0
$|c_{exp} - c_{sim}|/c_{exp}$ [-]
^{57}Co
^{60}Co
^{88}Y
^{109}Cd
^{137}Cs
^{133}Ba
^{152}Eu

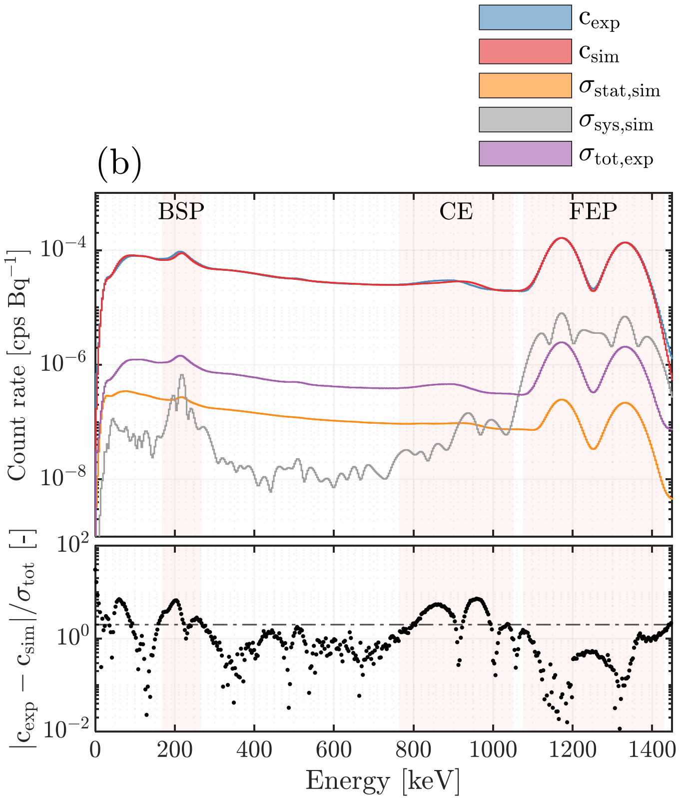

c_{exp}
c_{sim}
$\sigma_{stat,sim}$
$\sigma_{sys,sim}$
$\sigma_{tot,exp}$
(b)
BSP
CE
FEP
10^{-4}
10^{-6}
10^{-8}
Count rate [cps Bq^{-1}]
10^{2}
10^{0}
10^{-2}
$|c_{exp} - c_{sim}|/\sigma_{tot}$ [-]
0
200
400
600
800
1000
1200
1400
Energy [keV]

Appendix

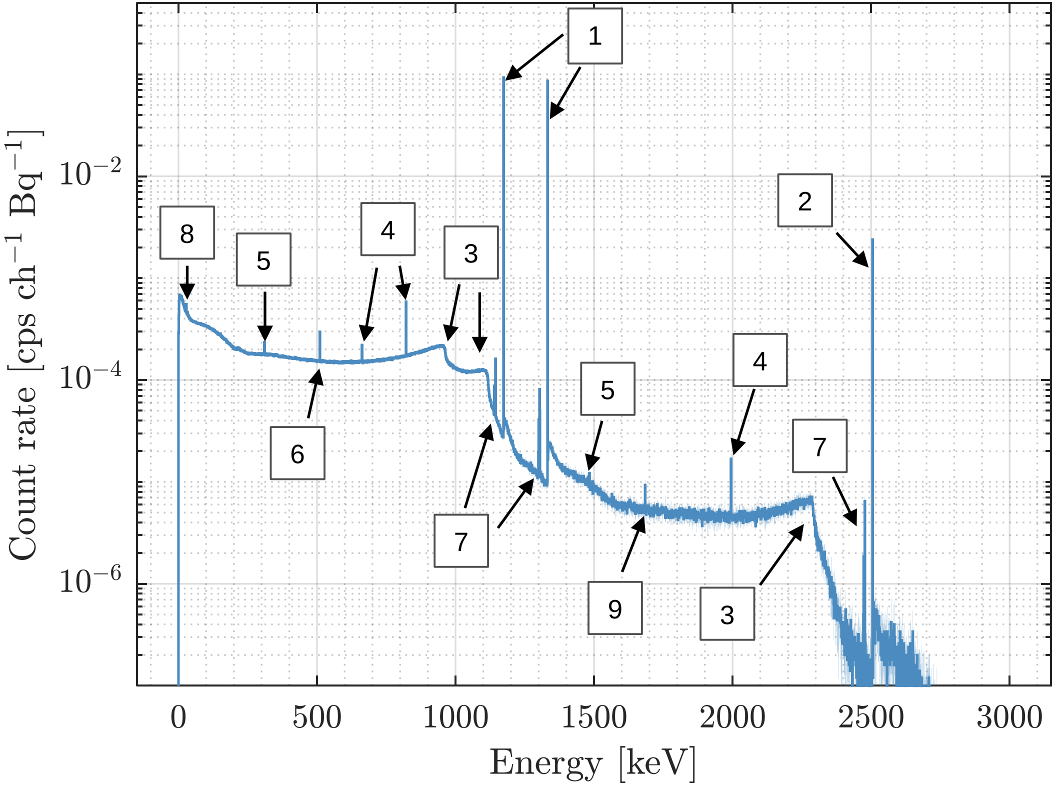

Fig. A-1 Simulated spectral gamma-ray response for Co-60 with simple model (only 4 detector crystals in air)

1. *Full energy peaks*
2. *True coincidence peak*
3. *Compton edges*
4. *Single-escape peaks*
5. *Double-escape peaks*
6. *Annihilation peak*
7. *Char. X-ray escape peak*
8. *Char. X-ray peak*
9. *Combined effects, e.g. annihilation & full energy peak*

Appendix

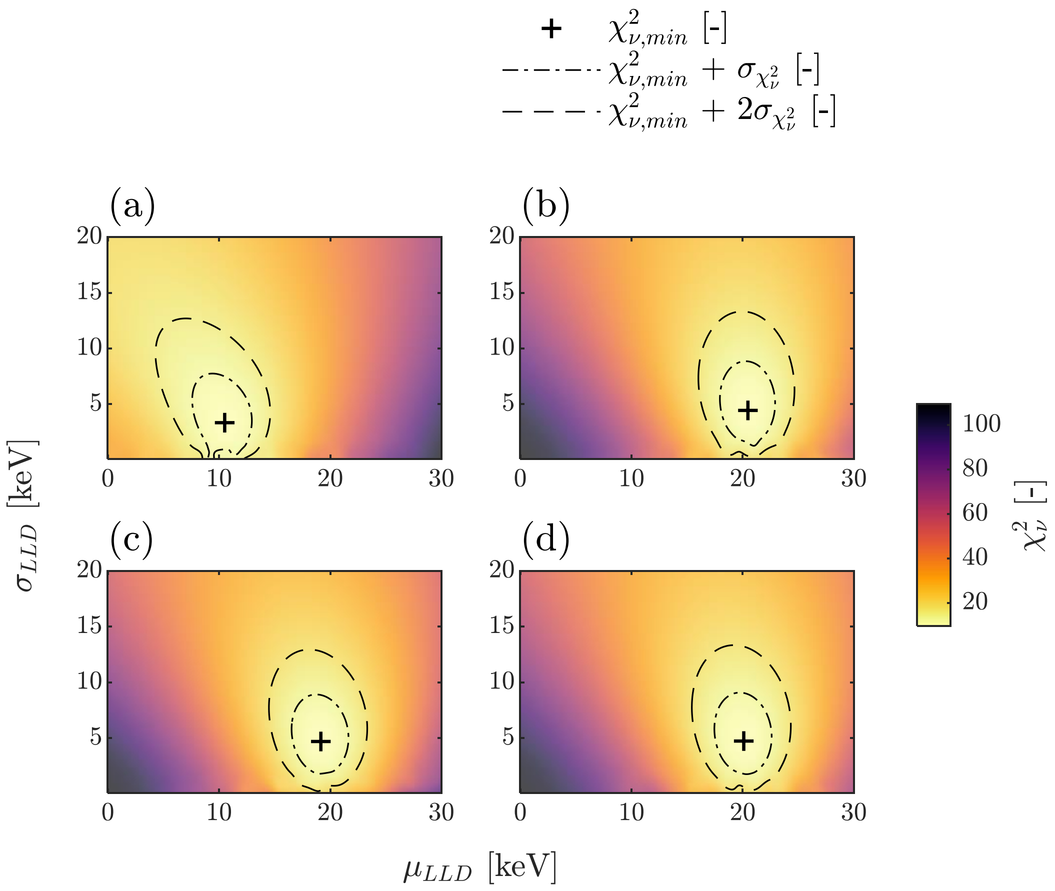

$\chi^2_{\nu,min}$ [-]
$\chi^2_{\nu,min} + \sigma_{\chi^2_\nu}$ [-]
$\chi^2_{\nu,min} + 2\sigma_{\chi^2_\nu}$ [-]
(a)
(b)
(c)
(d)
σ_{LLD} [keV]
μ_{LLD} [keV]
χ^2_ν [-]